

Spin- $\frac{1}{2}$ quantum antiferromagnets on the triangular lattice

P. W. Leung

*Supercomputer Computations Research Institute, Florida State University, Tallahassee, Florida 32306-4052
and Physics Department, The Hong Kong University of Science and Technology, Clear Water Bay, Hong Kong**

Karl J. Runge

*Physics Department, Lawrence Livermore National Laboratory, University of California, Livermore, California 94551
(Received 17 August 1992)*

The spin- $\frac{1}{2}$ anisotropic Heisenberg antiferromagnet is studied at $T = 0$ on the triangular lattice via numerical diagonalization for system sizes up to $N = 36$ sites. Extrapolation to the thermodynamic limit suggests that the isotropic system possesses no, or very small, $\sqrt{3} \times \sqrt{3}$ magnetic order; no helical or chiral order; and spin-spin correlations consistent with that of a critical phase. For XY -like anisotropy there is long-ranged $\sqrt{3} \times \sqrt{3}$ magnetic order. In contrast to bipartite lattices, the standard first- and second-order spin-wave theories are not quantitatively accurate. Excitation energy gaps suggest that the lowest-lying excitations for the isotropic point are not spin-flip excitations in the thermodynamic limit. The results for the isotropic point appear to agree with recent series expansion, large- N expansion, and the original resonating valence bond picture of Anderson, although they cannot be considered as conclusive evidence supporting any of these theories.

I. INTRODUCTION

The two-dimensional (2D) spin- $\frac{1}{2}$ Heisenberg antiferromagnet (HAF) has generated much interest in recent years. The Hamiltonian of the model is

$$\mathcal{H} = \sum_{\langle ij \rangle} \mathbf{S}_i \cdot \mathbf{S}_j, \quad (1.1)$$

where the sum is over the nearest neighbor pairs, and \mathbf{S}_i are spin- $\frac{1}{2}$ operators. The HAF on a square lattice¹ is believed to describe the undoped phase of the high- T_c superconductors² and is often used to describe the spin background of the doped phase, for example, in the t - J model. Through various approaches¹ it is now believed that the ground state of the square HAF has Néel ordering with staggered magnetization equal to about 60% of the classical value. It is well known that doping introduces frustration to the spin background, and this raises the possibility of describing the effect of doping by introducing frustration to the HAF. One such model is the frustrated HAF, in which one adds an antiferromagnetic coupling (J_2) to the next-nearest-neighbors on the square lattice. When the frustration is weak, the ground state still has Néel ordering. However, when the frustration is strong, the system decouples into two sublattices, each with Néel ordering. In the intermediate region, the system is believed to lose its Néel order. Various exotic states have been proposed, which include, among others, spin liquid,³ dimerized (spin-Peierls),⁴ twisted,⁵ and chiral-spin-liquid^{6,7} states. With frustration, it is difficult to do numerical studies via quantum Monte Carlo because of problems associated with minus signs. Therefore, more reliable numerical results come from the exact diagonalization study of finite clusters.^{8,9}

In addition to adding next-nearest-neighbor coupling, one can add frustration to the HAF geometrically. One example is the *kagomé* lattice. By far there is no concrete evidence that a spin liquid or other exotic state exists in the 2D HAF on any lattice, however, such states are most likely to be found in highly frustrated systems with large quantum fluctuations (small spin S and low coordination number). The *kagomé* HAF is attractive in this respect because it is highly frustrated, has a low coordination number and a large number of classically degenerate states.¹⁰ In fact, it has been suggested that the spin- $\frac{1}{2}$ *kagomé* HAF has a disordered ground state.¹¹⁻¹³ If so, then the *kagomé* HAF is one example where geometrical frustration alone can create a disordered ground state, without next-nearest-neighbor interaction. The triangular lattice also introduces frustration to the HAF. However, besides having a larger coordination number, it is well known that in the classical case the frustration can be partially released by arranging the spins at 120° to each other ($\sqrt{3} \times \sqrt{3}$ ordering),¹⁴ thereby retaining a Néel-type spin order. As a result, it seems a less likely candidate for having a disordered ground state. In fact, spin-wave theory¹⁵ (SWT) supports Néel ordering on the triangular lattice, but not on the *kagomé*.¹¹ Nevertheless, quite some time ago Anderson¹⁶ proposed the triangular HAF as a candidate for the resonating-valence-bond (RVB) state, which is a disordered spin liquid. RVB-type variational wave functions have been proposed⁵ and numerical studies¹⁷⁻¹⁹ also lend support to a disordered ground state. However, using a 120° Néel-type wave function, Huse and Elser²⁰ found that their variational energy is lower than that of the RVB-type wave functions. But recent work^{12,13} again points toward a disordered ground state, in particular, Singh and Huse¹² suggest the triangular HAF may be at, or at least very

close to, the critical point of losing magnetic order.

We ask the following question: Is the frustration in the spin- $\frac{1}{2}$ triangular HAF large enough to destroy the magnetic order? If so, is the ground state a spin liquid, or does it have some other form of long-range order (LRO)? In this paper, we study the triangular HAF using the exact diagonalization approach. Since first-order SWT supports Néel-type ordering, we also study the second-order SWT to see if the same conclusion holds and to compare with our numerical results. As mentioned above, due to the frustration, it is extremely difficult to use numerical methods like quantum Monte Carlo to study the triangular HAF, whereas the exact diagonalization approach gives numerically exact results for small finite clusters. Since the results inevitably suffer from finite-size effects, we have to study as large a system as we can and use finite-size extrapolation to infer the results in the thermodynamic limit. The largest system size we can diagonalize consists of $N = 36$ sites. Since it has been suggested¹² that the triangular HAF may be in some sense critical,²¹ we study a more general anisotropic Hamiltonian,

$$\mathcal{H} = \sum_{\langle ij \rangle} (S_i^x S_j^x + S_i^y S_j^y) + J_z \sum_{\langle ij \rangle} S_i^z S_j^z, \quad (1.2)$$

and attempt to observe any change of behavior as $J_z \rightarrow 1$. $J_z = 0$ corresponds to the triangular XY antiferromagnet (TXYAF), and $J_z = 1$ is the triangular Heisenberg antiferromagnet (THAF). Our results are consistent with the scenario that the system has $\sqrt{3} \times \sqrt{3}$ twisted magnetic LRO at $J_z = 0$, which decreases rapidly as J_z increases, and at $J_z = 1$ the LRO vanishes. This same pattern holds for the long-range helicity order parameter. For all $0 \leq J_z \leq 1$ there appears to be no chiral LRO. At $J_z = 1$ (THAF) the spin-spin correlation functions are consistent with power-law decay $\sim 1/r^x$ with $x = 1$, which agrees with the statement that this system may be nearly critical.^{12,22} The results of energy-gap calculations up to system size $N = 27$ are also consistent with the picture that the THAF is marginally losing its magnetic order. Summarizing, our results seem to imply that the THAF has a disordered ground state, and we did not find other kinds of LRO. As a result, they are consistent with the picture that the ground state of the THAF is a spin liquid with no broken symmetry^{6,13,16} (although we have not fully explored the possibility of long-range dimer order). However, we must caution that, due to small system-size limitations, we cannot rule out the possibility of the THAF having weak magnetic order. Indeed, it is difficult to rule out even 20% of the classical Néel value. The finite-size effect is especially serious in the energy-gap calculations, since we are not able to calculate the lowest-lying energy gaps of the $N = 36$ system. This paper is organized as follows. In Sec. II, we discuss the exact diagonalization method as applied to the present system under study. We interpret first the results for the spin-spin correlations in Sec. II A. Section II B contains our results for the twisted and sublattice magnetization long-range orders, followed by an interpretation of them in terms of the spin-wave theory in Sec. II C. Further physical properties are discussed in the follow-

ing sections: helicity long-range order (Sec. II D), chiral long-range order (Sec. II E), and energy gaps (Sec. II F); and, finally, Sec. III contains our conclusions.

II. NUMERICAL DIAGONALIZATION

We calculate the ground states of the TXYAF and THAF on triangular lattices of sizes $N = 9, 12, 21, 27,$ and 36 using the Lanczos algorithm.²³ All lattices used are hexagonal in shape with periodic boundary conditions (shown in Fig. 1), and the nearest-neighbor distance is 1. Where necessary, translational, C_{6v} , and spin reflection symmetries are used to reduce the number of basis states. More precisely, the C_{6v} operations we used are the three $\frac{2\pi}{3}$ rotations, and the reflections about the x and y axis, which together reduce the basis set roughly by a factor of 12. For even N , the ground state has $S_{\text{total}}^z = 0$, zero momentum and is symmetrical under all the C_{6v} operations (A_1 symmetry) and spin reflection. For odd N , the ground state has $S_{\text{total}}^z = \frac{1}{2}$ (or $-\frac{1}{2}$) and momentum $(\frac{4\pi}{3}, 0)$, is degenerate with positive and negative parities with respect to y reflection, and is symmetrical under all other C_{6v} operations. Using all the above symmetries, the $N = 36$ system has 10 524 036 states. The ground-state energies are tabulated in Table I. Assuming the finite-size correction for the energy goes as the linear SWT prediction (i.e., $1/N^{3/2}$), we find from $N = 12$ and 36 the ground-state energy per site²⁴ for the TXYAF to be $E/N = -0.4066$, and for the THAF, $E/N = -0.5485$. Note, however, that the SWT picture may not be valid for the THAF (see below in Secs. II B and II C). It is difficult to estimate the error in such an extrapolation. Using $N = 9$ and 27 yields values different from the above by 0.5% for the TXYAF and 1.0% for the THAF. We note that the extrapolation²⁵ for the (unfrustrated) square lattice HAF and XY model using $N = 16$ and 36 yields the exact answer to better than 0.1%. The values for the first-order (second-order) Holstein-Primakov SWT (Ref. 26) are -0.3992 (-0.4042) for the TXYAF

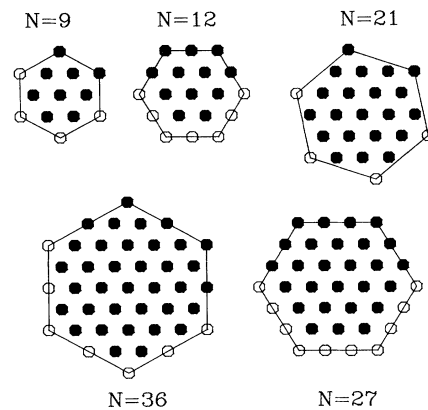


FIG. 1. The system sizes studied in this work. The filled symbols denote the triangular lattice sites of the system, while the open symbols are redundant and related to filled ones via cell translation vectors. The open symbols are included to illustrate the hexagonal shape of each cell.

TABLE I. Ground-state energies for the triangular antiferromagnets for various system sizes N and J_z . The last row is the ground-state energy per site in the thermodynamic limit obtained by extrapolating the $N = 12$ and 36 data.

N	$J_z=0.0$	$J_z=0.5$	$J_z=0.75$	$J_z=0.90$	$J_z=1.00$
9	-3.81703	-4.44191	-4.82743	-5.07723	-5.25000
12	-5.15024	-6.15600	-6.72558	-7.08164	-7.32396
21	-8.66998	-10.00912	-10.84375	-11.39494	-11.78091
27	-11.11577	-12.84395	-13.92086	-14.63012	-15.12597
36	-14.79446	-17.11317	-18.56203	-19.51156	-20.17344
E/N	-0.40661	-0.46640	-0.50492	-0.53051	-0.54847

and -0.5388 (-0.5468) for the THAF, and, therefore, our extrapolated values are quite close ($\sim 0.5\%$) to the second-order spin-wave predictions. We plot the first- and second-order spin-wave predictions along with our (even N) extrapolated values as a function of J_z in Fig. 2. The first few excited states can also be found using the Lanczos algorithm²⁷ and will be discussed in Sec. II F.

In the following sections, we will study the finite-size behavior of different order parameters. One difficulty of estimating finite-size corrections on the triangular antiferromagnet is that due to the limited system size and shape one can use, we have to use both even and odd N . We expect the even and odd results to extrapolate differently, although they should extrapolate to the same value in the thermodynamic limit. As a result, the number of data points we can use is rather small. Although we can do up to $N = 36$, we only have three data points for odd N and two for even N . This problem is less serious for quantities that extrapolate to “large” finite values, as in the case of the ground-state energy, but the problem is serious in those cases that extrapolate to very small values like some of the LRO parameters to be discussed in the following sections. For this reason, we do not attempt to fit our data to complicated and several-parameter functional forms as in Ref. 19. Instead, we

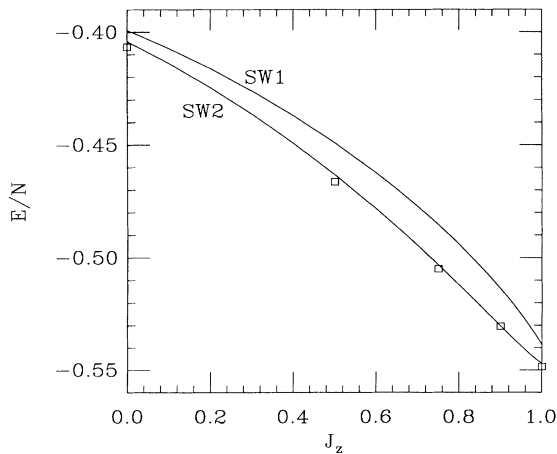


FIG. 2. Ground-state energy per site as a function of anisotropy parameter J_z for first-order spin-wave theory (SW1), second-order spin-wave theory (SW2), and from the extrapolation of the $N = 12, 36$ diagonalization results of the present work (\square).

shall mostly concentrate on deciding whether the thermodynamic limit is most likely zero or finite.

A. Spin-spin correlation function

A straightforward way to study the spin order is to examine how the spin-spin correlation in the z direction,

$$C^z(r) \equiv \langle S_0^z S_r^z \rangle, \quad (2.1)$$

behaves with increasing distance r . Spin-spin correlations for the triangular antiferromagnets are tabulated in Tables II and III. Results to be discussed in the following sections suggest the THAF does not have any magnetic LRO, which would imply $C^z(r)$ decays to zero at large r . If the THAF is a critical phase¹², then it is expected to be in the same universality class as the 3D stacked triangular lattice of classical Heisenberg spins, where the criticality is thermally driven and has been studied by Kawamura.²² For this $D = 3$ system, $\eta \simeq 0$, and therefore,

$$\begin{aligned} C^z(r) &\sim 1/r^{D-2+\eta} \\ &\sim 1/r. \end{aligned} \quad (2.2)$$

We take $C^z(\sqrt{3})$ from $N = 12$ and $C^z(3)$ from $N = 36$, each correspond to one of the extreme distances in the respective system size. Assuming the form $C^z(r) \sim 1/r^x$, we find $x = 0.96$, which is indeed close to 1. Perhaps this is evidence that the THAF is close to criticality. We remark that if the same procedure is used to fit to an exponential decay, $C^z(r) \sim \exp(-r/\xi)$, one finds a correlation length $\xi \approx 2.2$, which, although large for quantum spin systems, is not so large as to rule out this form. Larger system sizes could, of course, be used to distinguish between exponential and power-law behavior, but that probably will not be possible soon unless a quantum Monte Carlo scheme is developed to overcome the frustration minus sign problem for $N \sim 100 - 200$.

For $J_z < 1$, especially for small J_z , our results for the xy plane staggered spin-spin correlation function $C^{xy}(r)$ at large r are strongly suggestive that magnetic LRO exists. We define $C^{xy}(r)$ as

$$C^{xy}(r) \equiv n(0, \mathbf{r}) \langle S_0^x S_r^x \rangle, \quad (2.3)$$

where

$$n(\mathbf{r}_1, \mathbf{r}_2) = \begin{cases} 1 & \text{if } \mathbf{r}_1, \mathbf{r}_2 \in \text{same sublattice} \\ -2 & \text{otherwise.} \end{cases} \quad (2.4)$$

TABLE II. Correlation functions $\langle S_0^z S_n^z \rangle$ for the triangular antiferromagnets.

J_z	N	$n = 1$	$n = 2$	$n = 3$	$n = 4$	$n = 5$	$n = 6$
0.00	9	-0.03876	0.00517				
	12	-0.04878	0.02016	-0.00891			
	21	-0.03527	0.00139	-0.00447	-0.00400		
	27	-0.03521	-0.00195	-0.00343	-0.00298	-0.00136	
	36	-0.03518	0.00209	-0.00338	-0.00208	-0.00129	-0.00120
0.50	9	-0.05383	0.05037				
	12	-0.06135	0.04792	-0.01281			
	21	-0.04951	0.02371	-0.00903	-0.01457		
	27	-0.04975	0.02179	-0.00445	-0.01100	0.00989	
	36	-0.05028	0.02152	-0.00534	-0.00752	0.00879	0.00921
0.75	9	-0.06013	0.06929				
	12	-0.06504	0.05706	-0.01548			
	21	-0.05642	0.04149	-0.01678	-0.02393		
	27	-0.05653	0.03762	-0.01031	-0.01906	0.02446	
	36	-0.05688	0.03615	-0.01102	-0.01430	0.02208	0.02293
0.90	9	-0.06313	0.07827				
	12	-0.06679	0.06162	-0.01705			
	21	-0.06015	0.05247	-0.02216	-0.02953		
	27	-0.06014	0.04779	-0.01517	-0.02426	0.03498	
	36	-0.06027	0.04533	-0.01535	-0.01903	0.03158	0.03268
1.00	9	-0.06481	0.08333				
	12	-0.06781	0.06434	-0.01806			
	21	-0.06233	0.05916	-0.02555	-0.03288		
	27	-0.06225	0.05414	-0.01845	-0.02750	0.04179	
	36	-0.06226	0.05115	-0.01826	-0.02214	0.03787	0.03914

The factor n adjusts for the $\cos(120^\circ) = -1/2$ between different sublattices. A plot of $C^{xy}(r)$ for the TXYAF is shown in Fig. 3, and one can see that the LRO is apparent.

B. Magnetic ordering

A relevant order parameter for the $\sqrt{3} \times \sqrt{3}$ magnetic order for the anisotropic triangular antiferromagnets is the twisted magnetization^{18,19} defined by

$$N_I = \sum_{j \in A} S_j^x + \sum_{j \in B} S_j^y + \sum_{j \in C} S_j^z, \quad (2.5)$$

where A , B , and C denote the sublattices, and

$$S_j^u = -\frac{1}{2} S_j^x + \frac{\sqrt{3}}{2} S_j^y, \quad (2.6)$$

$$S_j^v = -\frac{1}{2} S_j^x - \frac{\sqrt{3}}{2} S_j^y. \quad (2.7)$$

These quantities are spin projections along directions rotated $\pm 120^\circ$ from the x axis, and point along the directions of a classical Néel state. The mean square of the twisted magnetization can be calculated from the two-spin correlation functions,

$$\langle N_I^2 \rangle = N \left(\frac{1}{4} + \sum_{r \in A'} \langle S_0^x S_r^x \rangle - \sum_{r \in B} \langle S_0^x S_r^x \rangle \right), \quad (2.8)$$

TABLE III. Correlation functions $\langle S_0^z S_n^z \rangle$ for the triangular antiferromagnets.

J_z	N	$n = 1$	$n = 2$	$n = 3$	$n = 4$	$n = 5$	$n = 6$
0.00	9	-0.07069	0.12241				
	12	-0.07153	0.09695	-0.03924			
	21	-0.06881	0.11070	-0.05389	-0.05490		
	27	-0.06862	0.10832	-0.05167	-0.05291	0.10321	
	36	-0.06849	0.10722	-0.05136	-0.05105	0.10131	0.10057
0.50	9	-0.06880	0.09982				
	12	-0.07016	0.07381	-0.02282			
	21	-0.06706	0.08293	-0.03831	-0.04327		
	27	-0.06685	0.07857	-0.03307	-0.03900	0.06945	
	36	-0.06666	0.07515	-0.03201	-0.03458	0.06507	0.06570
0.75	9	-0.06685	0.09036				
	12	-0.06902	0.06820	-0.01975			
	21	-0.06491	0.06928	-0.03088	-0.03756		
	27	-0.06473	0.06421	-0.02420	-0.03239	0.05303	
	36	-0.06461	0.06060	-0.02341	-0.02713	0.04846	0.04970
0.90	9	-0.06562	0.08586				
	12	-0.06830	0.06573	-0.01862			
	21	-0.06337	0.06268	-0.02738	-0.03458		
	27	-0.06325	0.05756	-0.02031	-0.02920	0.04555	
	36	-0.06321	0.05433	-0.01992	-0.02384	0.04138	0.04269

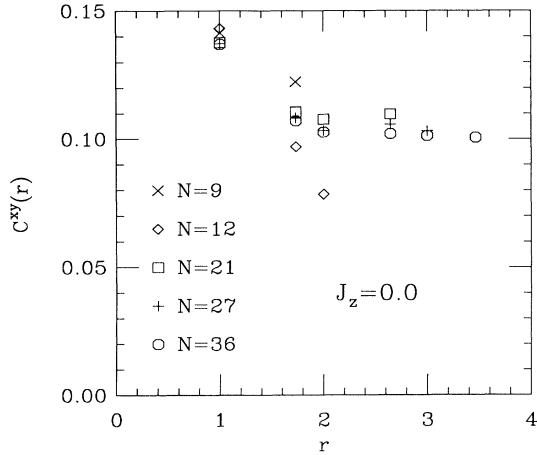


FIG. 3. Spin-spin correlation function $C^{xy}(r)$ vs r for the TXYAF at various system sizes.

where site 0 is taken to be in sublattice A , and A' means sublattice A excluding site 0. Nishimori and Nakanishi¹⁹ (NN) calculated the twisted magnetization for the TXYAF and THAF for system sizes up to $N = 27$. They concluded that the twisted magnetization LRO decays by a power law for the TXYAF and decays exponentially for the THAF, in other words, neither system has magnetic ordering as $N \rightarrow \infty$. However, they did remark that their system sizes were too small to draw definite conclusions about the nonexistence of LRO in the THAF.

We calculate the twisted magnetization for $J_z = 0, 0.5, 0.75, 0.9, \text{ and } 1$. The results are plotted in Fig. 4, where the abscissa was selected based on linear spin-wave theory, in which case the quantity $\langle N_1^2 \rangle / N^2$ would fall in a straight line, for large N . For $J_z = 0$ (TXYAF), it is obvious that the even and odd N results follow different curves. If we assume that both converge to the same value as $N \rightarrow \infty$, it is clear that this value is finite,

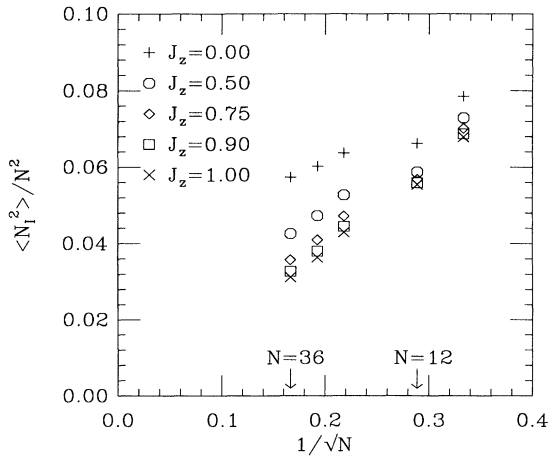


FIG. 4. The size dependence of the twisted magnetization LRO parameter for the various J_z .

roughly 0.04 to 0.045. This implies that the TXYAF has magnetic LRO, and with a value consistent with a series-expansion calculation.²⁸ Although we cannot say what the exact form of extrapolation should be, the finite value is in sharp contrast with NN.¹⁹ We believe that it is dangerous to fit to functional forms with a few parameters when the number of data points is limited. By taking into account the even N points ($N = 12$ and 36), we believe that the twisted magnetization has finite ordering. The above value corresponds to a twisted magnetization equal to $82\% \pm 3\%$ of the classical 120° Néel state, and should be contrasted with the linear spin-wave theory prediction of 90% (see below). As J_z increases, the extrapolated value decreases rapidly. Furthermore, the even and odd N results seem to collapse to a single curve as J_z approaches 1. At $J_z = 1$ (THAF), all the data points almost fall on a straight line. The even and odd N results may still have different curvatures for these small N , although they are both small. If we extrapolate the two points $N = 12$ and 36 linearly in $1/\sqrt{N}$ to $N = \infty$, we get -0.0018 . This small negative value suggests that the twisted magnetization is zero for the THAF in the thermodynamic limit. Note that if the THAF is critical, then $C^x(r) \sim 1/r$ from Sec. II A, and we expect the quantity $\langle N_1^2 \rangle / N^2$ to scale as the inverse of the linear dimension, that is to say, also²⁹ $1/\sqrt{N}$. The fact that the THAF $N = 12$ and 36 points extrapolate linearly to a value close to zero is consistent with the critical phase correlation functions. Nevertheless, we cannot say conclusively that $\langle N_1^2 \rangle / N^2$ for the THAF does not take on a small value as $N \rightarrow \infty$.

In analogy with the square lattice HAF, one can define the staggered magnetization m^\dagger for the THAF, which is also a relevant order parameter for the $\sqrt{3} \times \sqrt{3}$ magnetic order. It can be defined in terms of the asymptotic behavior of the staggered spin-spin correlation

$$C(\mathbf{r}) = \frac{1}{N} \sum_{\mathbf{R}} n(\mathbf{R}, \mathbf{R} + \mathbf{r}) \langle \mathbf{S}_{\mathbf{R}} \cdot \mathbf{S}_{\mathbf{R} + \mathbf{r}} \rangle, \quad (2.9)$$

where $n(\mathbf{R}, \mathbf{R} + \mathbf{r})$ is defined in Eq. (2.4). The staggered magnetization m^\dagger can be calculated from

$$m^{\dagger 2} = C(\mathbf{r}_{\max}), \quad (2.10)$$

where \mathbf{r}_{\max} is the maximum separation in the hexagonal cell with periodic boundary conditions. Since there are two distinct extreme distances r_a and r_b in a hexagonal cell, we define two estimates for m^\dagger in terms of $C(\mathbf{r})$,

$$m_1^2 = C(\mathbf{r}_a), \quad (2.11a)$$

$$m_2^2 = C(\mathbf{r}_b). \quad (2.11b)$$

We can define two other estimates for m^\dagger , one in terms of the sublattice magnetization

$$m_3^2 = \frac{3}{(N/3)^2} \sum_{ij \in A} \langle S_i^z S_j^z \rangle, \quad (2.11c)$$

and the other one by removing the self term in Eq. (2.11c),

$$m_4^2 = \frac{3}{(N/3-1)} \sum_{r \in A'} \langle S_0^z S_r^z \rangle. \quad (2.11d)$$

All of these quantities are, of course, directly related to the twisted magnetization: LRO in one implies LRO in the others. These quantities can be calculated easily from Tables II and III. We plot them in Fig. 5. The linear SWT result¹⁵ of 48% of the classical value is also shown in the graph. We note that for m_3^2 , the even and odd N results also lie on a single line. Extrapolation of the $N = 12$ and 36 results gives -0.0036 . This small negative value again indicates that the infinite-size staggered magnetization is very close to zero. While the other estimates may converge to larger values, their even and odd N results lie on very different curves, thus making the extrapolation difficult. One would need a very large system size to see those trends clearly. These results emphasize the subtlety of extracting the thermodynamic limit of m^\dagger from the $N \leq 36$ data for the THAF.

In the anisotropic case we define the sublattice magnetization as

$$m^{\dagger 2} = \frac{2}{(N/3)^2} \sum_{ij \in A} \langle S_i^x S_j^x \rangle, \quad (2.12)$$

since no LRO is expected in the $\langle S_i^z S_j^z \rangle$ correlations. The finite-size dependence of this quantity is shown in Fig. 6.

C. Spin-wave theory comparison

Over the last several years, a large body of work^{1,25,30-32} has revealed the somewhat surprising result that in two-dimensions (and higher) and for all spins the standard spin-wave theory^{1,33-35} is a remarkably accurate theory for the energy and LRO parameter of bipartite lattice Heisenberg antiferromagnets. This also holds for anisotropic *ferromagnets*³⁶ (including the non-bipartite triangular lattice²⁵). For example, the spin- $\frac{1}{2}$,

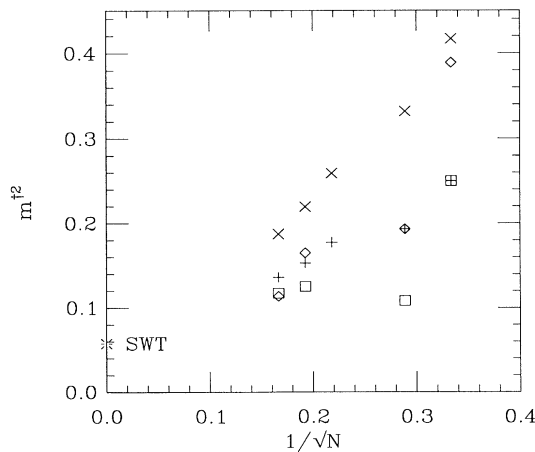


FIG. 5. The size dependence of the various estimates for the staggered magnetization of the THAF. The symbols are (\diamond) m_1^2 , (\square) m_2^2 , (\times) m_3^2 , and ($+$) m_4^2 . The spin-wave theory (SWT) result is also shown.

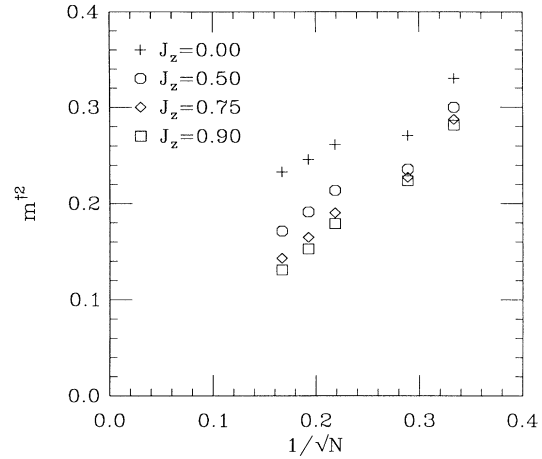


FIG. 6. The finite-size extrapolation of the sublattice magnetization LRO parameter for the various J_z .

square lattice HAF second-order spin-wave predictions are within 0.15% and 1.3% of the “exact” results for the ground-state energy and LRO parameter, respectively.³⁷ The agreement is even better for the spin- $\frac{1}{2}$ XY ferromagnet. One might guess that the good quantitative agreement will result for nonbipartite lattices as well; however, we feel this is not the case and believe that frustration effects (geometrical or otherwise) play an important role in spoiling the accuracy of the theory. We shall show this below for the case of the nearest-neighbor triangular antiferromagnets.

In spin-wave theory (SWT) one expands about the $S = \infty$ (or classical) limit, which for the triangular lattice antiferromagnets is the 120° Néel state. We take the LRO to lie in the xy plane. Following Miyake^{26,38} we define a spatially varying coordinate system x' , y' , z' , with z' pointing along the local 120° Néel direction and y' pointing along the old z direction. $\sigma_i^x, \sigma_i^y, \sigma_i^z$ will be the spin operator components along x', y', z' , respectively. Specifically,

$$\sigma_i^z = \begin{cases} S_i^x & \text{if } i \in A \\ -\frac{1}{2}S_i^x + \frac{\sqrt{3}}{2}S_i^y & \text{if } i \in B \\ -\frac{1}{2}S_i^x - \frac{\sqrt{3}}{2}S_i^y & \text{if } i \in C, \end{cases} \quad (2.13)$$

where the $\sigma_i^x, \sigma_i^y, \sigma_i^z$ are spin S operators, that is to say, they obey the standard angular momentum commutation relations and $(\sigma^x)^2 + (\sigma^y)^2 + (\sigma^z)^2 = S(S+1)$.

The Hamiltonian may now be exactly expressed as

$$H = -\frac{1}{2} \sum_{\langle ij \rangle} [\sigma_i^z \sigma_j^z + \sigma_i^x \sigma_j^x] + J_z \sum_{\langle ij \rangle} \sigma_i^y \sigma_j^y + \sum_{\langle ij \rangle} \sin(\phi_{ij}) [\sigma_i^x \sigma_j^z - \sigma_i^z \sigma_j^x] \quad (2.14)$$

$$= H_1 + H_2 + H_3, \quad (2.15)$$

where ϕ_{ij} is the difference in classical Néel angles between sites i and j : $\sin(\phi_{ij}) = \pm\sqrt{3}/2$ for nearest neighbors. Note that on bipartite lattices, $\sin(\phi_{ij}) = 0$, and so the third “currentlike” term H_3 is absent: Its presence above

is entirely due to geometrical frustration. The term H_1 is the standard ferromagnetic one, although due to frustration its amplitude is reduced by $|\cos(\phi_{ij})| = 1/2$.

In the Holstein-Primakov transformation one expresses the spin operators σ in terms of site magnon deviation operators:

$$\sigma_i^z = S - n_i, \quad (2.16)$$

$$\sigma_i^+ = \sqrt{2S - n_i} a_i, \quad (2.17)$$

$$\sigma_i^- = a_i^\dagger \sqrt{2S - n_i}, \quad (2.18)$$

where $\sigma_i^\pm = \sigma_i^x \pm i\sigma_i^y$, $n_i = a_i^\dagger a_i$, and a_i^\dagger, a_i are boson creation and annihilation operators. The transformation in Eq. (2.13) is convenient in that it avoids the introduction of different magnon operators for each of the three sublattices. One next expands the square roots in the operators under the assumption that the ‘‘magnon deviations’’ $\langle n_i/2S \rangle$ are small and collects the terms in a power series in $1/S$. The lowest-order contributions are

$$H_1^{(1)} = -\frac{N\nu}{4}S^2 + \frac{1}{2}S\nu \sum_i n_i - \frac{1}{4} \left(\frac{\sqrt{2S}}{2} \right)^2 \sum_{i\delta} (a_i^\dagger + a_i)(a_{i+\delta}^\dagger + a_{i+\delta}), \quad (2.19)$$

$$H_2^{(1)} = -\frac{J_z}{2} \left(\frac{\sqrt{2S}}{2} \right)^2 \sum_{i\delta} (a_i^\dagger - a_i)(a_{i+\delta}^\dagger - a_{i+\delta}), \quad (2.20)$$

$$H_3^{(1)} = -\frac{\sqrt{2S}}{2} \sum_{i\delta} \sin \phi_{i\delta} (a_i^\dagger + a_i) n_{i+\delta}, \quad (2.21)$$

where $\nu = 6$ is the number of nearest neighbors, and δ denotes the nearest neighbors of site i . Note that $H_1^{(1)}$ also includes the ‘‘zeroth-order’’ term $-(N\nu/4)S^2$, which is the energy of the classical 120° Néel state. It is also useful to add a term that couples the 120° Néel magnetization ($= \sum_i \sigma_i^z$) to a field h , which we write as

$$H_4 = H_4^{(1)} = h \sum_i (S - \sigma_i^z) = h \sum_i n_i, \quad (2.22)$$

since the LRO parameter is then given by

$$m^\dagger = S - \frac{1}{N} \frac{\partial E}{\partial h}, \quad (2.23)$$

where E is the ground-state energy of the system.

The first-order spin-wave results are readily obtained by diagonalizing the quadratic Hamiltonian $H_{\text{SW1}} = H_1^{(1)} + H_2^{(1)} + H_4^{(1)}$ via the standard Bogoliubov transformation.³⁵ This yields the coefficient of order S of the ground-state energy, and m^\dagger is then found by differentiating with respect to h . The resulting expressions for E and m^\dagger are straightforward sums over the Brillouin zone. For spin- $\frac{1}{2}$, one can easily find that the energy is $E^{(1)}/N = -0.3992$ and the LRO parameter $m^{\dagger(1)} = 0.4485$ ($\approx 90\%$) for the case of the TXYAF, and $E^{(1)}/N = -0.5388$ and $m^{\dagger(1)} = 0.2387$ ($\approx 48\%$) for the

THAF. In the latter case, we regain the results of Ref. 15, which were obtained in a more complicated manner that does not utilize the transformation in Eq. (2.13).

Note that the three magnon ‘‘geometrical-frustration’’ term $H_3^{(1)}$ does not contribute at first order. Since the coefficient of $H_3^{(1)}$ is \sqrt{S} , one might first guess that it provides an energy correction of order \sqrt{S} ; however this is not so because the three magnon expectation value in the ground state of H_{SW1} vanishes (see the discussion below). We feel it has not been stressed enough in the literature that the first-order spin-wave (SW1) predictions for triangular (and other frustrated) antiferromagnets is equivalent to the same treatment of a *ferromagnet with no H_3 term*. That is to say, it is equivalent to the first-order spin-wave calculation applied to the Hamiltonian³⁹

$$H' = -1/2 \sum [\sigma_i^z \sigma_j^z + \sigma_i^x \sigma_j^x] + J_z \sum \sigma_i^y \sigma_j^y. \quad (2.24)$$

Thus for the frustrated TXYAF (i.e., $J_z = 0$) the SW1 results are precisely the same as for the completely unfrustrated triangular lattice XY ferromagnet. Within spin-wave theory, the difference between the two systems only arises at second order and beyond. The spin- $\frac{1}{2}$ triangular lattice XY ferromagnet has been shown by quantum Monte Carlo²⁵ and series expansions³⁰ to have LRO parameter m^\dagger within 1% of the SW1 (and second-order spin-wave theory) predictions, while the result for the TXYAF found in the present work (81%) appears distinct from the SW1 (90%) prediction. We feel the difference increases as $J_z \rightarrow 1$, since the frustration effect increases. Evidence for the trend is displayed in Fig. 7, where we plot the finite-size ($N = 12, 36$) extrapolations of the sublattice magnetization [Eq. (2.12)] for $J_z = 0.0, 0.5, 0.75$, and 0.90 along with the spin-wave theory results. From the figure, the discrepancy between the finite N extrapolated value and the SW1 result evidently increases with J_z .

The second-order spin-wave (SW2) contributions (of

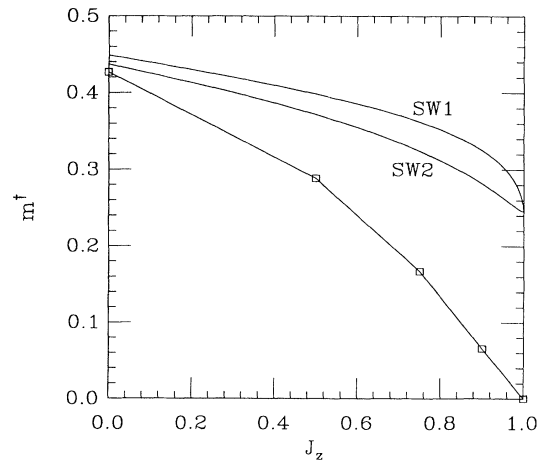


FIG. 7. Comparison of the $N = 12, 36$ extrapolated m^\dagger of the present work (\square) to the first- and second-order spin-wave results (SW1 and SW2, respectively) as a function of anisotropy J_z .

order S^0 in the energy) arise from two sources: (1) the standard³⁵ second-order piece from H^1 defined above and (2) the contribution from $H_3^{(1)}$. We will call these contributions $\delta E_{(1+2)}^{(2)}$ and $\delta E_3^{(2)}$, respectively. We discuss the $\delta E_3^{(2)}$ contribution, since it is somewhat unfamiliar.²⁶ The product of three magnon operators means the expectation value of $H_3^{(1)}$ vanishes in the Boboliubov ground state: $\langle \text{SW1} | H_3^{(1)} | \text{SW1} \rangle = 0$, so it must be treated in higher-order perturbation theory. The second-order perturbation result is

$$\delta E_3^{(2)} = \sum_{\{n_{\mathbf{k}}\}} \frac{|\langle \{n_{\mathbf{k}}\} | H_3^{(1)} | \{0\} \rangle|^2}{E(\{0\}) - E(\{n_{\mathbf{k}}\})}, \quad (2.25)$$

where $|\{n_{\mathbf{k}}\}\rangle$ is an eigenstate of the quadratic (i.e., SW1) Hamiltonian with magnon occupation numbers denoted by $\{n_{\mathbf{k}}\}$. $E(\{n_{\mathbf{k}}\})$ is the corresponding energy and is given by $\sum_{\mathbf{k}} (n_{\mathbf{k}} + 1/2) \hbar \omega_{\mathbf{k}}$. $|\{0\}\rangle$ denotes the ground state with no magnons present, and $\hbar \omega_{\mathbf{k}}$ is the SW1 magnon spectrum given by

$$\hbar \omega_{\mathbf{k}} = \frac{1}{2} \nu S [(1 - \gamma_{\mathbf{k}})(1 + 2J_z \gamma_{\mathbf{k}})]^{1/2} \quad (2.26)$$

[where $\gamma_{\mathbf{k}} = (1/\nu) \sum_{\delta} \exp(i\mathbf{k} \cdot \delta)$] when the applied magnetic field h is zero. Note that, since $H_3^{(1)}$ is proportional to \sqrt{S} and $\omega_{\mathbf{k}}$ is proportional to S , the contribution $\delta E_3^{(2)}$ is indeed of order S^0 . The primary contribution in Eq. (2.25) is from states with three magnons present and reduces to a double sum over the Brillouin zone.

The calculation of m^\dagger within SW2 for the THAF has only recently appeared in the literature.³⁸ There it was found that the SW2 correction actually slightly *increases* the value of m^\dagger from 48% to 50%. We have verified and applied Miyake's³⁸ formula to the case $J_z < 1$. For the TXYAF we find m^\dagger is reduced slightly from $m^{\dagger(1)} = 0.4485$ to $m^{\dagger(2)} = 0.4367$, and so makes up some, but evidently not all, of the diagonalization estimate $m^\dagger = 0.405 \pm 0.02$. We note in passing that the SW2 correction to m^\dagger is about 40 times smaller for the triangular spin- $\frac{1}{2}$ XY ferromagnet than for the TXYAF, and, hence, the H_3 contribution is the dominate one for the TXYAF. As seen in Fig. 7, the deviation of the spin-wave results from the diagonalization predictions grows quickly with J_z .

D. Helicity

It is well known that the classical $\sqrt{3} \times \sqrt{3}$ structure has an Ising-like variable¹⁴ associated with each triangular

plaquette, which we call helicity. Classically, it is found that helicity LRO exists at zero temperature, and gives rise to a Kosterlitz-Thouless type of phase transition at finite temperature.⁴⁰ For $S = \frac{1}{2}$, such a transition seems to be suppressed,⁴¹ perhaps by quantum fluctuations. It is interesting to see if quantum fluctuations destroy the helicity LRO in the ground state.

Following Fujiki and Betts,¹⁸ we define the helicity operator for each triangle as

$$\begin{aligned} H_i^z &\equiv \frac{2}{\sqrt{3}} (\mathbf{S}_1 \times \mathbf{S}_2 + \mathbf{S}_2 \times \mathbf{S}_3 + \mathbf{S}_3 \times \mathbf{S}_1)^z \\ &= \frac{1}{\sqrt{3}i} [(S_1^- S_2^+ - S_1^+ S_2^-) + (S_2^- S_3^+ - S_2^+ S_3^-) \\ &\quad + (S_3^- S_1^+ - S_3^+ S_1^-)], \end{aligned} \quad (2.27)$$

where the sites 1, 2, and 3 are taken in a clockwise sense around the triangle. The eigenvalues of H_i^z are ± 1 and 0. To investigate the long-range helicity order, we define the quantity

$$H \equiv \sum_{i \in \Delta} H_i^z, \quad (2.28)$$

where the sum is over the upright triangles. NN (Ref. 19) calculated the helicity (they called it "chirality") LRO for the TXYAF and THAF up to $N = 27$. They concluded that the helicity LRO decays by a power law for the TXYAF, and decays exponentially for the THAF, and so, once again, they predict no such LRO as $N \rightarrow \infty$ for either system.

Our helicity results are tabulated in Table IV and plotted in Fig. 8. For the TXYAF, the even and odd N results seem to follow different curves with opposite curvature. If we assume that both extrapolate to the same value as $N \rightarrow \infty$, they obviously extrapolate to a finite value, which is about 0.58. This again contradicts the results of NN.¹⁹ For the THAF, the even and odd N results almost fall on the same curve, which seems to extrapolate to zero or a small number as $N \rightarrow \infty$. Thus we believe that the TXYAF has helicity LRO, while the THAF does not.

E. Chirality

As discussed before, the nature of the ground state of the THAF has generated much controversy. Kalmeyer and Laughlin⁶ have proposed a RVB state that breaks chiral symmetry as the ground state for the THAF. It

TABLE IV. Helicity LRO $\langle H^2 \rangle / N^2$ for various system sizes N and anisotropies J_z .

J_z	$N = 9$	$N = 12$	$N = 21$	$N = 27$	$N = 36$
0.00	0.69462	0.58122	0.61427	0.59703	0.58781
0.50	0.60890	0.45870	0.46442	0.42159	0.38498
0.75	0.54895	0.41983	0.36202	0.30971	0.26801
0.90	0.51485	0.40069	0.30575	0.25233	0.21371
1.00	0.49383	0.38926	0.27391	0.22156	0.18536

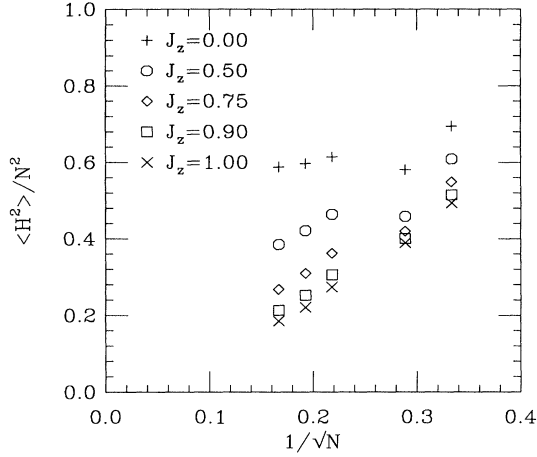


FIG. 8. The size dependence of the helicity LRO parameter for TXYAF (+) and THAF (\times), and intermediate J_z (see legend).

is known that nonzero expectation values of the operator $\mathbf{S}_1 \cdot (\mathbf{S}_2 \times \mathbf{S}_3)$ implies chiral symmetry breaking.⁷ Baskaran⁴² has shown that chiral symmetry breaking should be enhanced by next-nearest-neighbor interaction. However, a numerical study by Imada⁴³ did not show evidence of chiral symmetry breaking for the THAF with nearest-neighbor interaction, consistent with recent prediction based on large- N expansion.¹³ A finite-size study ($N = 21$) by Deutscher *et al.*⁴⁴ did not show enhancement in the chiral order parameter even in the presence of next-nearest-neighbor interaction.

Consider a plaquette of four spins as shown in Fig. 9, we define the uniform chiral operator $X_i^{(+)}$ and the staggered chiral operator $X_i^{(-)}$ for plaquette i to be

$$X_i^{(+)} \equiv \frac{2}{\sqrt{3}} [\mathbf{S}_1 \cdot (\mathbf{S}_2 \times \mathbf{S}_3) + \mathbf{S}_2 \cdot (\mathbf{S}_4 \times \mathbf{S}_3)], \quad (2.29)$$

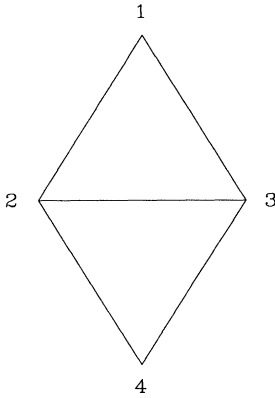


FIG. 9. A plaquette of four spins on which the uniform and staggered chiral operators are defined.

$$X_i^{(-)} \equiv \sqrt{2} [\mathbf{S}_1 \cdot (\mathbf{S}_2 \times \mathbf{S}_3) - \mathbf{S}_2 \cdot (\mathbf{S}_4 \times \mathbf{S}_3)]. \quad (2.30)$$

The normalizations are chosen such that the maximum magnitudes of the eigenvalues are 1 in both cases. The uniform chirality X_+ and the staggered chirality X_- are defined as

$$X_+ \equiv \sum_i X_i^{(+)}, \quad (2.31)$$

$$X_- \equiv \sum_i X_i^{(-)}. \quad (2.32)$$

The results are tabulated in Table V. The uniform chiral LRO parameter of both the TXYAF and THAF are plotted in Fig. 10. Both appear to extrapolate to zero, in agreement with Ref. 43, where a different kind of extrapolation scheme is used. The staggered chiral LRO of the THAF are plotted in Fig. 11. They are much smaller than the uniform one and seem to suggest zero as $N \rightarrow \infty$.

F. Energy gaps for the THAF

Energy gaps can be important in studying long range order. For the THAF, we consider the magnetic order, where the appropriate energy gap is the spin-flip gap. Those excitations generated by spin-flip operations have higher S_{total} than the ground state. If these excitations are gapless, i.e., the lowest-energy state with higher S_{total} is degenerate with the ground state in the thermodynamic limit, then magnetic LRO should exist. In the thermodynamic limit, the ground state is a singlet and the lowest spin-flip excitation is a triplet. Therefore, one should consider the singlet-singlet gap (the energy difference between the ground state and the first excited singlet state) and the singlet-triplet gap (the energy difference between the ground state and the lowest triplet state). It is well known that in the square HAF, both the singlet-singlet gap and the singlet-triplet gap go to zero in the thermodynamic limit, with, however, the singlet-triplet gap much smaller than the singlet-singlet gap, i.e., the lowest-lying excitations are spin-flip excitations. Anderson¹⁶ conjectured that in the THAF the singlet-triplet gap is finite, while the singlet-singlet gap is zero. However, numerical results of Sütő and Fazekas⁴⁵ suggested that both singlet-triplet and singlet-singlet gaps vanish in the thermodynamic limit. Therefore, both singlet and triplet low-lying excitations are present.

TABLE V. Chirality LRO for the TXYAF and THAF for various system sizes N .

N	TXYAF	THAF	
	$\langle X_+^2 \rangle / N^2$	$\langle X_+^2 \rangle / N^2$	$\langle X_-^2 \rangle / N^2$
9	0.05534	0.07128	0.05238
12	0.07905	0.10246	0.00008
21	0.02526	0.03815	0.00872
27	0.01998	0.03149	0.00548
36	0.01502	0.02465	0.00280

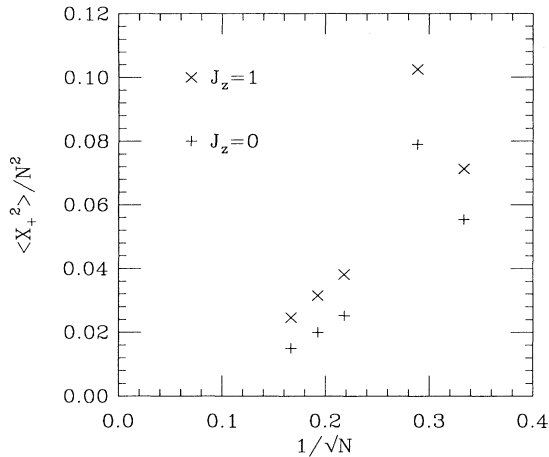


FIG. 10. The size dependence of the uniform chirality LRO parameter for TXYAF (+) and THAF (x).

Since some of the small clusters we are dealing with have odd N , singlet and triplet states do not exist, and we have to study the doublet-doublet and doublet-quartet gaps in those cases. In Table VI we tabulate the first few lowest-energy states for the THAF up to $N = 27$. For $N = 9$, the ground state is a doublet. The first excited doublet state is degenerate with the lowest quartet state. For both $N = 12$ and 21, the first excited state is the spin-flip state, i.e., having a higher S_{total} than the ground state. The first excited state, which has the same S_{total} as the ground state, is the third excited state. For $N = 27$, the spin-flip excitation is no longer the lowest excited state. There is a doublet state between the ground state and the lowest quartet state. This level crossing of the first excited state with system size shows the complex nature of the excitation spectrum as compared to the unfrustrated square lattice HAF. In Fig. 12 we plot the doublet and quartet gaps for odd N . The former is the gap between the ground state (which is a doublet) and

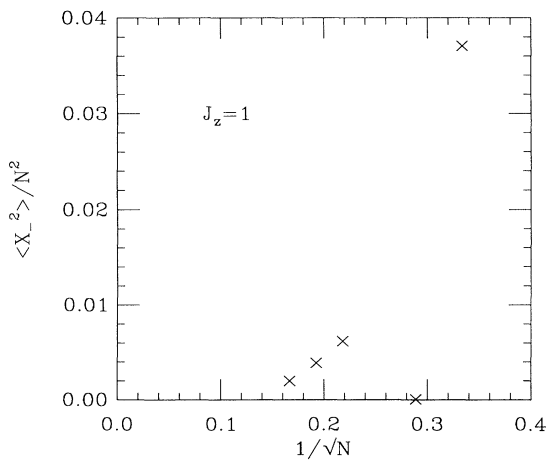


FIG. 11. The size dependence of the staggered chirality LRO parameter for THAF.

TABLE VI. Ground states and the first few excited states of the THAF for various system sizes N .

N	Energy	S_{total}	Momentum
9	-5.2500	1/2	$(4\pi/3, 0)$
	-3.7500	3/2	$(0, 0)$
	-3.7500	3/2	$(4\pi/3, 0)$
	-3.7500	1/2	$(2\pi/3, 2\pi/3\sqrt{3})$
12	-7.3240	0	$(0, 0)$
	-6.4608	1	$(4\pi/3, 0)$
	-6.4272	1	$(0, 0)$
	-6.3700	0	$(0, 0)$
21	-11.7809	1/2	$(4\pi/3, 0)$
	-11.0785	3/2	$(0, 0)$
	-11.0628	3/2	$(4\pi/3, 0)$
	-11.0606	1/2	$(4\pi/7, -8\pi/7\sqrt{3})$
27	-15.1260	1/2	$(4\pi/3, 0)$
	-14.6117	1/2	$(8\pi/9, 0)$
	-14.5298	3/2	$(0, 0)$
	-14.5235	3/2	$(4\pi/3, 0)$

the first excited doublet, and the latter is the gap between the ground state and the lowest quartet. We find that the smallest excitation gap (the smaller of the doublet and quartet gap) appears to extrapolate linearly to zero, while the spin-flip excitation gap (quartet gap) seems to extrapolate to a small but finite value.⁴⁶ If this scenario is correct, namely, the spin-flip excitation has a gap, and the excitation with the same S_{total} as the ground state is gapless, then the THAF does not possess magnetic LRO (which agrees with our interpretations in Sec. II B), and there may exist other kinds of LRO. But we have to caution that the above speculation depends heavily on the small N results and may also be influenced by the fact that odd N has been used. As always, it is dangerous to infer the large N behavior from a limited number of data points at small N . Spin gaps for $N = 36$ will be

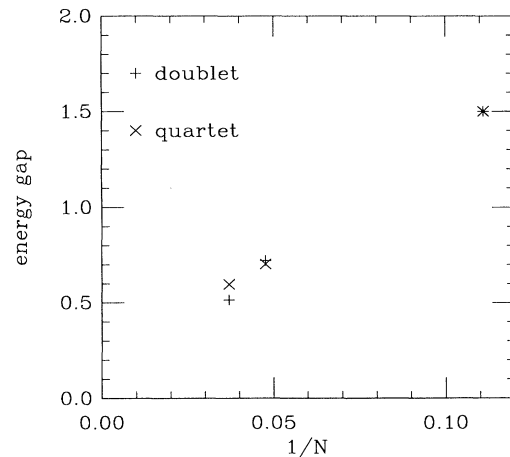


FIG. 12. The size dependence of the doublet (+) and quartet (x) gaps for odd N for the THAF.

much more convincing. Unfortunately, we are not able to calculate the lowest-lying spin-flip gaps for $N = 36$ at the present time. However, it does seem possible from our results that the spin-flip excitations are not the lowest excitation at large N .

The THAF is in sharp contrast with the simple nature of the excitation spectrum of the square HAF, where the spin-flip excitation is gapless and therefore magnetic LRO exists.¹ This simple picture can be complicated by adding frustration to the square HAF. From the finite cluster study of the frustrated square HAF,⁸ it is found that singlet states exist between the ground state and the lowest triplet state for a certain range of J_2/J_1 , and the system does not possess antiferromagnetic LRO. Geometrical frustration in the THAF seems to produce the same effect. The *kagomé* HAF, which is another example of geometrical frustration, also has a similar picture. The lowest excitation of the *kagomé* HAF has the same S_{total} as the ground state.⁴⁷ We therefore believe that the geometrical frustration in the triangular lattice is enough to destroy the magnetic spin order. One difference between the gap structures of the *kagomé* and triangular HAF is that the first excited states always have the same S_{total} as the ground state in the *kagomé* HAF, whereas this does not happen except for larger N in the THAF. This may suggest that the *kagomé* HAF loses its magnetic LRO in a more drastic manner than the THAF, and may also bolster the idea that the THAF is marginally close to losing its magnetic LRO.

III. CONCLUSION

To summarize, we have calculated the ground states of the TXYAF and THAF with system sizes $N = 9, 12, 21, 27,$ and 36 by exact diagonalization.⁴⁸ We study those possible long-range orders, which are most often associated with the triangular antiferromagnets, namely, magnetic order, helicity and chirality. The kind of magnetic order we look for is a Néel type ordering with $\sqrt{3} \times \sqrt{3}$ unit cells.¹⁴ Using finite-size extrapolations, we infer the existence or nonexistence of these orderings in the thermodynamic limit. Due to the small number of system sizes we have and the fact that even and odd N results often lie on different curves, precise extrapolation is not feasible, and we are not always able to extract accurate estimates for these quantities in the thermodynamic limit. Finally, we study the spin gaps for magnetic order.

For the TXYAF, our results strongly suggest the existence of magnetic and helicity LRO, but not chiral LRO. Thus we have shown that quantum fluctuations in the ground state of the spin- $\frac{1}{2}$ system are not sufficient to destroy the magnetic and helicity LRO, which also exist in the classical ground state. This is contrary to NN (Ref. 19) who studied the same quantities with the same approach, but included system sizes up to $N = 27$ only. By fitting their data to different functional forms, they concluded that both the twisted magnetization and the helicity LRO decayed to zero via power laws. By adding the $N = 36$ results, we believe that we can rule out

their power-law fits in both cases. However, in a later publication,¹⁹ they did remark that their system sizes are too small to draw definite conclusions. The LRO that exists for the TXYAF should persist for a nonzero range of J_z about zero.

For the THAF, although we cannot definitely rule out the existence of magnetic LRO, our results do suggest that it does not exist. Of the four different estimates for the staggered magnetization defined in Eqs. (2.11a)–(2.11d), m_3^2 has the most obvious, and perhaps most reliable trend for extrapolation. Extrapolation of m_3^2 suggests that even if the staggered magnetization in the thermodynamic limit is not zero, it should be a good deal smaller than the linear SWT result of 48% of the classical value. This is in agreement with the series expansion calculations of Singh and Huse.¹² Similarly, the helicity and chirality LRO are inferred not to exist. Spin-gap calculations show that spin-flip excitations are not the lowest-lying excitations for large N . Although this supports the picture that the THAF does not possess magnetic LRO, it is somewhat ambiguous because this is the case for $N = 27$ only, and we are not able to do the same for $N = 36$. It will be much more convincing if one can show that the lowest-lying excitations for $N = 36$ are not spin-flip excitations. By studying $0 < J_z < 1$, we found that the extrapolated twisted magnetization decreases rapidly with increasing J_z . Spin-spin correlations are consistent with the speculation that the THAF may be in the critical phase of losing its spin order, which was suggested from the series expansion work.¹² Overall, our results seem to support the speculation that the THAF is a spin-liquid with no broken symmetry, which is consistent with the original RVB conjecture¹⁶ and large- N expansion (for “sufficiently small” spin).¹³ A recent experiment⁴⁹ also seems to imply that the THAF has no magnetic order at low temperature. Although we must admit that our results cannot be taken as conclusive evidence for the above-mentioned picture, we believe that they are enough to cast doubt on the belief that the spin- $\frac{1}{2}$ THAF possesses Néel-type ordering. If one does assume this conclusion, it immediately poses intriguing questions: (1) Is the spin- $\frac{1}{2}$ THAF a spin-liquid, and, if not, what is the form of the LRO? (2) What is the critical value of the spin S_c ($> 1/2$) at which the Néel order is regained for the THAF?

Finally, we remark that the 36-site system is the biggest we can handle at present, yet it still seems too small for performing finite-size extrapolation, especially when the quantity we are studying may be zero in the thermodynamic limit. This comes as no surprise: If the THAF is really in the critical phase of losing its spin order,¹² then one should expect very serious finite-size effects. By looking at the scaling plots, one will be convinced that even $N = 48$ results cannot add much information. The properties of that system are, however, much more difficult to obtain by diagonalization than the $N = 36$ results, and we do not expect it to be possible in the near future. Therefore, we feel that a quantum Monte Carlo approach that can deal with the negative sign problem is needed to draw more definite conclusion to the present problem.

ACKNOWLEDGMENTS

We thank V. Elser, R. J. Gooding, D. A. Huse, and R. R. P. Singh for helpful discussions. P.W.L. was supported by the Florida State University Supercomputer Computations Research Institute (SCRI), which is partially funded by the U.S. Department of Energy through

Contract No. DE-FC05-85ER25000. K.J.R. was supported by Lawrence Livermore National Laboratory under U.S. Department of Energy Contract No. W-4705-Eng-48. The numerical diagonalizations were performed on the Thinking Machines Corporation Connection Machine CM-2 at SCRI.

*Present address.

- ¹E. Manousakis, *Rev. Mod. Phys.* **63**, 1 (1991), and references therein.
- ²S. Chakravarty, D. Nelson, and B. I. Halperin, *Phys. Rev. Lett.* **60**, 1057 (1988); S. Chakravarty, B. I. Halperin, and D. Nelson, *Phys. Rev. B* **39**, 2344 (1989).
- ³P. Chandra and B. Doucot, *Phys. Rev. B* **38**, 9335 (1988); F. Figueirido, A. Karlhede, S. Kivelson, S. Sondhi, M. Rocek, and D. S. Rokhsar, *ibid.* **41**, 4619 (1990).
- ⁴N. Read and S. Sachdev, *Phys. Rev. Lett.* **62**, 1694 (1989); M. P. Gelfand, R. R. P. Singh, and D. A. Huse, *Phys. Rev. B* **40**, 10801 (1989).
- ⁵P. Chandra, P. Coleman, and A. Larkins, *Phys. Rev. Lett.* **64**, 88 (1990).
- ⁶V. Kalmeyer and R. B. Laughlin, *Phys. Rev. Lett.* **59**, 2095 (1987).
- ⁷X. G. Wen, F. Wilczek, and A. Zee, *Phys. Rev. B* **39**, 11413 (1989).
- ⁸E. Dagotto and A. Moreo, *Phys. Rev. B* **39**, 4744 (1989); H. J. Schultz and T. A. L. Ziman, *Europhys. Lett.* **18**, 355 (1992).
- ⁹D. Poilblanc, E. Gagliano, S. Bacci, and Dagotto, *Phys. Rev. B* **43**, 10970 (1991).
- ¹⁰C. Broholm, G. Aeppli, G. P. Espinosa, and A. S. Cooper, *Phys. Rev. Lett.* **65**, 3173 (1990); A. B. Harris, C. Kallin, and A. J. Berlinsky, *Phys. Rev. B* **45**, 2899 (1992).
- ¹¹C. Zeng and V. Elser, *Phys. Rev. B* **42**, 8436 (1990).
- ¹²R. R. P. Singh and D. A. Huse, *Phys. Rev. Lett.* **68**, 1766 (1992).
- ¹³S. Sachdev, *Phys. Rev. B* **45**, 12377 (1992).
- ¹⁴J. Villain, *J. Phys. (Paris)* **38**, 385 (1977).
- ¹⁵Th. Jolicœur and J. C. Le Guillou, *Phys. Rev. B* **40**, 2727 (1989).
- ¹⁶P. W. Anderson, *Mater. Res. Bull.* **8**, 153 (1973); P. Fazekas and P. W. Anderson, *Philos. Mag.* **30**, 423 (1974).
- ¹⁷T. Oguchi, H. Nishimori, and Y. Taguchi, *J. Phys. Soc. Jpn.* **55**, 323 (1986).
- ¹⁸S. Fujiki and D. D. Betts, *Can. J. Phys.* **65**, 76 (1987); S. Fujiki, *ibid.* **65**, 489 (1987).
- ¹⁹H. Nishimori and H. Nakanishi, *J. Phys. Soc. Jpn.* **57**, 626 (1988); **58**, 2607 (1989); **58**, 3433 (1989).
- ²⁰D. A. Huse and V. Elser, *Phys. Rev. Lett.* **60**, 2531 (1988).
- ²¹Where, for example, the spin-spin correlation function would exhibit power-law decay.
- ²²H. Kawamura, *J. Appl. Phys.* **63**, 3086 (1988); *Phys. Rev. B* **38**, 4916 (1988); *J. Phys. Soc. Jpn.* **58**, 584 (1989).
- ²³J. K. Cullum and R. A. Willoughby, *Lanczos Algorithms for Large Symmetric Eigenvalue Computations* (Birkhauser, Boston, 1985). For the implementation of the Lanczos algorithm on the Connection Machine CM2, see P. W. Leung and P. E. Oppenheimer, *Comp. Phys.* (to be published).
- ²⁴As happens in the square lattice case, the odd and even N results probably have differing *subleading* finite-size energy corrections, e.g., α/N^2 , with different α for odd and even N .
- ²⁵S. Zhang and K. J. Runge, *Phys. Rev. B* **45**, 1052 (1992); K. J. Runge *Phys. Rev. B* **45**, 7229 (1992); **45**, 12292 (1992).
- ²⁶S. J. Miyake *Prog. Theor. Phys.* **74**, 468 (1985).
- ²⁷J. Cullum and R. A. Willoughby, *J. Comput. Phys.* **44**, 329 (1981).
- ²⁸R. R. P. Singh (private communication).
- ²⁹Due to this property we feel it is somewhat safer to extrapolate $\langle N_i^2 \rangle / N^2$ and $m^{\dagger 2}$ rather than the square roots of these quantities.
- ³⁰W. H. Zheng, J. Oitmaa, and C. J. Hamer, *Phys. Rev. B* **43**, 8321 (1991); C. J. Hamer, J. Oitmaa, and W. H. Zheng, *ibid.* **43**, 10789 (1991); J. Oitmaa, C. J. Hamer, and W. H. Zheng, *ibid.* **45**, 9834 (1992).
- ³¹R. R. P. Singh, *Phys. Rev. B* **39**, 9760 (1989); R. R. P. Singh and D. A. Huse, *ibid.* **40**, 7247 (1989).
- ³²J. D. Reger and A. P. Young, *Phys. Rev. B* **37**, 5978 (1988).
- ³³P. W. Anderson, *Phys. Rev.* **86**, 694 (1952).
- ³⁴R. Kubo, *Phys. Rev.* **87**, 568 (1952); T. Oguchi, *Phys. Rev.* **117**, 117 (1960).
- ³⁵W. H. Zheng, J. Oitmaa, and C. J. Hamer, *Phys. Rev. B* **44**, 11869 (1991), and references therein.
- ³⁶These statements are made for systems with nearest-neighbor interactions only, but in some cases may apply to more general situations.
- ³⁷In fact, there is evidence that the third-order spin-wave results make up much of the remaining difference for the square lattice HAF; S. M. Girvin and C. Canali (private communication).
- ³⁸S. J. Miyake *J. Phys. Soc. Jpn.* **61**, 983 (1992). We thank R. J. Gooding for pointing out this reference. Our derivations agree with the formula in Eq. 10d of this reference. The same quantity in Eq. 4.4b of Ref. 26 appears to contain a typographical error.
- ³⁹ H' does, of course, have antiferromagnetic tendencies from the $J_z \sigma_i^y \sigma_j^y$ term, but the (classically) dominate terms are ferromagnetic.
- ⁴⁰S. Miyashita and H. Shiba, *J. Phys. Soc. Jpn.* **53**, 1145 (1984); D. H. Lee, J. D. Joannopoulos, J. W. Negele, and D. P. Landau, *Phys. Rev. Lett.* **52**, 433 (1984); H. Kawamura and S. Miyashita, *J. Phys. Soc. Jpn.* **53**, 4138 (1984).
- ⁴¹M. Imada, *J. Phys. Soc. Jpn.* **56**, 311 (1987).
- ⁴²G. Baskaran, *Phys. Rev. Lett.* **63**, 2524 (1989).
- ⁴³M. Imada, *J. Phys. Soc. Jpn.* **58**, 2650 (1989).
- ⁴⁴R. Deutscher, H. U. Everts, S. Miyashita, and M. Wintel, *J. Phys. A* **23**, L1043 (1990).
- ⁴⁵A. Sütő and P. Fazekas, *Philos. Mag.* **35**, 623 (1977).
- ⁴⁶This picture is further supported when the $N = 3$ data is included (not shown in Fig. 12).
- ⁴⁷C. C. Wan (unpublished); P. W. Leung and V. Elser (unpublished).

⁴⁸We note that we recently saw work by Bernu, Lhuillier, and Pierre (unpublished) in which they have also diagonalized the $N = 36$ for the THAF case but claim that magnetic LRO exists.

⁴⁹K. Takeda, K. Miyake, K. Takeda, and K. Hirakawa, *J. Phys. Soc. Jpn.* **61**, 2156 (1992). We thank R. J. Gooding for pointing out this reference.